Journal of Sustainability for Energy
https://www.acadlore.com/journals/JSE

Influence of Cavity Geometry on Thermo-Fluid Transport and Freshwater Productivity in a Solar Still: A Numerical Study

A. Rezvani Nasab*, S. Khodami, M. J. Sarmadi

Department of Mechanical Engineering, Babol Noshirvani University of Technology, 47148-71167 Babol, Iran

* Correspondence: A. Rezvani Nasab (ali.rezvani@stu.nit.ac.ir)

Received: 03-03-2026 **Revised:** 03-31-2026 **Accepted:** 04-10-2026

Citation: A. Rezvani Nasab, S. Khodami, and M. J. Sarmadi, "Influence of cavity geometry on thermo-fluid transport and freshwater productivity in a solar still: A numerical study," *J. Sustain. Energy*, vol. 5, no. 2, pp. 109–119, 2026. https://doi.org/10.56578/jse050202.

Abstract: The cavity geometry of a single-slope solar still directly influences the internal transport phenomena by altering natural convection, heat transfer, and vapor movement, as their alteration collectively determines the system's freshwater productivity. Variations in the glass cover inclination modify the cavity geometry, thereby changing the natural convection flow pattern, evaporation, and condensation mechanisms, as well as the overall thermal behavior of the solar still. Despite its importance, the impact of cavity geometry on the internal transport phenomena has not yet been fully understood. Therefore, the present work conducted a systematic two-dimensional numerical investigation to assess the effects of five glass cover inclination angles (10°, 15°, 20°, 25°, and 30°) on the thermo-fluid behavior and freshwater productivity. To isolate the influence of cavity geometry, the basin length and front-wall height were kept constant, while the back-wall height was varied to produce the desired inclination angles without altering the remaining design parameters. The numerical results confirmed that modifying the glass cover inclination induced a substantial change in the natural convection flow regime within the still cavity, leading to significant nuances in heat and mass transfer characteristics. At steeper inclination angles, the airflow was dominated by a single large recirculating convection cell that confined convective heat transfer between the evaporating water surface and the glass cover, causing a uniform reduction in the effectiveness of condensation and freshwater production. In contrast, the shallowest inclination angle of 10° promoted the formation of multiple localized convection cells that enhanced fluid mixing, strengthened convective heat transfer, and improved vapor transport toward the condensing surface. Consequently, the 10° configuration exhibited the highest freshwater productivity among all investigated geometries.

Keywords: Single-slope solar still; Natural convection; Numerical simulation; Glass cover inclination; Solar desalination; Freshwater productivity

1 Introduction

Access to clean and sufficient water resources is essential for sustaining human life and supporting socioeconomic development. However, rapid population growth, industrial expansion, and increasing water consumption have intensified the pressure on limited freshwater resources, hence creating significant barriers in meeting global water demands. To fulfil these expectations, numerous desalination methods have been employed. Conventional methods are highly energy-intensive and reliant on fossil fuels. The concerted effort of solar stills offer a solution by transforming saline water into fresh and clean water using an eco-friendly approach. Solar stills are especially useful in places that are arid and desert regions, which suffer from a lack of conventional water supplies but are sun-exposed all year round [1, 2]. Elango and Murugavel [3] investigated the use of glass as a basin material to boost solar still productivity. The performance of insulated and uninsulated solar stills was experimentally investigated, showing that the double-basin double-slope configuration consistently surpassed the single-basin design. Interestingly, a shallow basin water depth of 1 cm was identified as the most favorable condition for achieving maximum efficiency in both systems. Under the climatic conditions of Rewa in central India, Agrawal et al. [4] carried out a combined theoretical and experimental study to analyze the thermal behavior and performance of a single-slope basin-type solar still. Theoretical and experimental analyses conducted for basin water depths between 2 cm and 10 cm reflected that an increase in water depth weakened the evaporation process by minimizing the water temperature, evaporative heat transfer coefficient, and both instantaneous and cumulative distillate production. Furthermore, the strong correlation between the calculated and measured results highlighted the capability of the theoretical model to accurately predict the performance of the solar still. Johnson et al. [5] studied a theoretical model simulating the effect of an external solar enhancement on the productivity in the New Mexico region. To improve solar energy absorption and increase the available thermal energy for evaporation, a point-focusing Fresnel lens was utilized. This could assist in achieving a substantial rise in the productivity of the still and discover that using Frensel lens becomes more effective at larger water depths.

Kabeel et al. [6] conducted experimental investigations of a solar still incorporating an internal reflector and thermal heat storage system, where the effects of pure phase change material (solar still with phase change material, SS-PCM) and paraffin wax–black gravel composite storage (solar still with composite material, SS-CM) were compared. The scholars revealed that replacing part of the pure phase change material with black gravel provided an economic advantage, to lower the freshwater production cost by about 27%. Thakur et al. [7] employed a nanoparticle-based modification strategy to enhance solar still performance by adding nanoparticles to the basin water and examining the improvement in freshwater production compared with a conventional design. Their analysis showed that nanoparticle-assisted operation improved solar still productivity with CuO and ZnO nanofluids, resulting in freshwater yield enhancements of 41.6% and 11.11%, respectively, compared with the conventional configuration. Nagaraju et al. [8] explored the use of sand troughs as a passive enhancement technique for a single-slope solar still, aiming to improve heat storage characteristics and increase freshwater production. They argued that the sand trough-assisted configuration achieved superior thermal performance, compared with the conventional design, with improvements of 71.4% in daily productivity and an overall efficiency reaching 65.08%. To increase the evaporation surface area of a single-slope solar still, Hameed et al. [9] proposed a novel absorbent base consisting of stainless-steel geometries with different shapes and sizes. These stainless-steel geometries, in application, helped enhance the evaporation rate as well as the productivity of the solar still. Changing size significantly increased the water yield, ultimately achieving a 38.2% improvement when utilizing cone shapes. Saad et al. [10] examined the effect of incorporating three different phase change materials into a single-slope solar still with an internal reflector and experimentally assessed their impact on freshwater productivity. Soy wax was found to be the most productive and inexpensive option, increasing the total yield up to 124.74% in the spring season and lowering the production cost per liter to $0.041. Abdelgaleel et al. [11] proposed a modified solar still incorporating iron hemispherical pieces (IHPs) and steel wool pads (SWPs) and analyzed their effects on thermal performance and freshwater production. The study demonstrated that optimal performance occurred at a lower water volume, while larger basin volumes significantly decreased productivity. They indicated that optimizing the system configuration substantially improved the overall performance of the modified solar still, resulting in maximum exergy efficiency of 3.5%. El-Sebaey et al. [12] introduced a novel stepped-basin tubular solar still (SBTSS) that optimized performance by reducing the equivalent water depth. The SBTSS attained a maximum daily yield of 3,826 mL/m^2, outperforming a conventional tubular still. The stepped design increased overall productivity, while lowering the water production cost to $0.0159 per liter and with a payback period of 124 days.

Although prior numerical and experimental studies have evaluated the performance of single-slope solar stills, most have primarily focused on enhancing freshwater productivity through modifications such as basin materials, phase change materials, nanoparticles, external condensers, and solar collectors. In contrast, comparatively limited attention has been devoted to understanding the fundamental influence of cavity geometry on the internal thermo-fluid dynamics that govern evaporation and condensation processes. In particular, the role of glass cover inclination in governing the internal natural convection regime, the spatial distribution of heat and mass transfer, and the condensation process within the cavity has not been systematically examined, leaving a notable gap in the understanding of thermo-fluid transport in single-slope solar stills. Previous studies, in general, evaluated productivity improvements at a limited number of inclination angles or under varying geometric and operating conditions, rendering it difficult to isolate the specific contribution of cavity geometry. The physical mechanisms responsible for the changes in freshwater productivity based on variations in glass cover inclination remain insufficiently explored. Accordingly, this work presented a detailed two-dimensional numerical analysis of a single-slope solar still with five different glass cover inclinations between 10° and 30°. The geometric influence is isolated by fixing the basin length and front-wall height and by varying only the back-wall height to produce the desired cavity configurations. This approach enabled the geometric influence to be examined independently of other design parameters, providing an explicit understanding of the relationship between cavity configuration and thermo-fluid behavior. The study went beyond evaluating freshwater productivity by analyzing the evolution of natural convection patterns, circulation cells, temperature fields, and local convective heat transfer within the solar still cavity. Such a detailed investigation contributed to new insights into how geometric modifications altered the internal transport phenomena responsible for evaporation and condensation. The principal novelty of this work lied in confirming the existence of a geometry-dependent transition in the internal flow regime as the glass cover inclination changed. Specifically, the study demonstrated that reducing the inclination angle promoted the formation of multiple localized convection cells, whereas steeper configurations were characterized by a single dominant circulation loop. This transition directly affected the local heat transfer distribution and vapor transport pathways, ultimately determining the freshwater productivity of the solar still. By systematically relating cavity geometry to the internal flow regime and the associated heat and mass transfer characteristics, the present study offered a mechanistic understanding of solar still operation that went beyond traditional productivity assessments and laid a more robust scientific basis for future geometric optimization. The outcomes of this work were valuable scientific and engineering contributions for the design and optimization of passive solar desalination systems. The findings established a clearer physical basis for selecting appropriate glass cover geometries to maximize thermal performance and freshwater production without increasing system complexity or energy consumption. Not surprisingly, the findings of this work supported the development of more efficient and sustainable solar desalination systems by initiating design plans that could enhance freshwater production in water-scarce and remote areas with limited access to conventional energy infrastructure.

2 Computational Domain and Physical Model

The system under investigation was a single-slope solar still, which was computationally evaluated. It consisted of a basin containing saline water that was enclosed with adiabatic walls to prevent heat loss and topped with an inclined transparent glass cover (see Figure 1). The glass cover served multiple purposes as it transmitted solar radiation to heat the saline water, thereby driving surface evaporation and simultaneously acting as a heat sink where the ascending vapor condensed. To isolate the effects of slope inclination, the basin length and the front wall height were fixed at 0.5 m and 0.1 m, respectively. To evaluate five distinct inclination angles ranging from 10° to 30°, the back wall height increased and intentionally expanded the volume of the water vapor cavity providing domain variations to analyze. A mixture of dry air and water vapor moved inside the domain, and its movement was driven by temperature gradients and solutal buoyancy between the water and glass. The water and glass surfaces were active walls modeled as isothermal boundaries; the water surface acted as a heat source at a higher constant temperature while the glass surface served as a heat sink at a lower constant temperature. The evaporation and condensation interfaces were assumed to be fully saturated and side walls were impermeable to mass fraction. As shown in Figure 1, five different cases have been simulated in present work based on the temperature of glass and water.

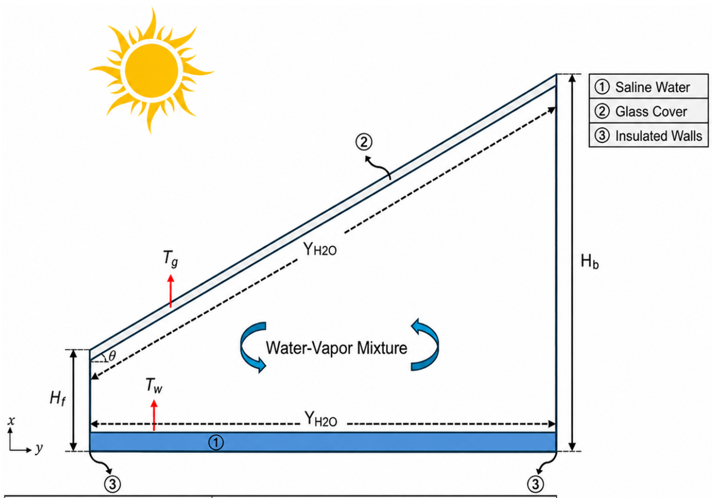

	Case1	Case2	Case3	Case4	Case5
Water Temperature (K)	336.15	336.15	336.15	336.15	336.15
Glass Temperature (K)	321.15	321.15	321.15	321.15	321.15

Figure 1. Two-dimensional computational domain and applied boundary conditions

The governing equations are as follows [13, 14]:

$$\frac{\partial u}{\partial x}+\frac{\partial v}{\partial y}=0 \tag{1}$$

$$u\frac{\partial u}{\partial x}+v\frac{\partial v}{\partial y}=-\frac{1}{\rho}\frac{\partial p}{\partial x}+v\left(\frac{\partial^2 u}{\partial x^2}+\frac{\partial^2 u}{\partial y^2}\right) \tag{2}$$

$$\rho\cong\rho_0-\rho_0\beta\left(T-T_0\right)-\rho_0\beta^*\left(C-C_0\right),\beta=-\frac{1}{\rho}\left(\frac{\partial\rho}{\partial T}\right)_p,\beta^*=-\frac{1}{\rho}\left(\frac{\partial\rho}{\partial C}\right)_p \tag{3}$$

$$u\frac{\partial v}{\partial x}+v\frac{\partial v}{\partial y}=-\frac{1}{\rho}\frac{\partial p}{\partial y}+v\left(\frac{\partial^2 v}{\partial x^2}+\frac{\partial^2 v}{\partial y^2}\right)+\beta g\left(T-T_0\right)-\beta^*\left(C-C_0\right) \tag{4}$$

$$u\frac{\partial T}{\partial x}+v\frac{\partial T}{\partial y}=\alpha\left(\frac{\partial^2 T}{\partial x^2}+\frac{\partial^2 T}{\partial y^2}\right) \tag{5}$$

where, x and y are Cartesian coordinates (m), u and v are velocity components (m/s). The term p represents pressure (Pa), ρ is density (kg/m^3), and β is the thermal expansion coefficient (K^{-1}). Furthermore, T is temperature (K), C is concentration (kg/m^3), g is gravitational acceleration (m/s^2), and α is thermal diffusivity (m^2/s).

Boundary condition could be summarized as follows: At the glass surface: $T = T_{\text{glass}}$; at the water surface: $T = T_{\text{water}}$; at water-vapor interface and glass-vapor interface, air is assumed to be saturated ($\phi = 100\%$, ϕ represents relative humidity); at side walls: $\frac{\partial T}{\partial x} = 0$, $\frac{\partial C}{\partial x} = 0, u = 0, v = 0$.

To calculate the amount of fresh water, the definition below could be adopted [15]:

$$\dot{m}=-\frac{D_m}{L}\int_0^L \left.\frac{\partial C}{\partial y}\right|_{\text{water}} \mathrm{d}x \tag{6}$$

where, $\dot{m}$ is mass productivity $(\mathrm{kg/m^2 \cdot s})$, D_m is mass diffusivity (m^2/s), and L represents the basin length (m).

As illustrated in the computational framework, the numerical investigation began with the development of a two-dimensional computational geometry representing the single-slope solar still (Figure 2). The conservation equations associated with momentum, energy, and species transport were solved using the finite volume formulation of ANSYS Fluent to predict the coupled heat and mass transfer behavior inside the solar still cavity. Before performing the final simulations, a mesh independence analysis was conducted to ensure that the obtained results were not influenced by the computational grid resolution. For this purpose, the mesh was progressively refined, and the key output parameters were monitored until negligible variations were observed between successive mesh levels. The mesh configuration, providing an acceptable balance between computational accuracy and numerical efficiency, was then selected for all subsequent simulations. After establishing the appropriate mesh resolution, the solver settings and discretization schemes were defined. The PRESTO! scheme was employed for pressure interpolation due to its suitability for buoyancy-driven flows involving strong pressure gradients. Second-order upwind discretization schemes were adopted for the momentum, energy, and species transport equations to enhance solution accuracy and minimize numerical diffusion. These numerical settings guaranteed a reliable prediction of the natural convection flow field, temperature distribution, and water vapor transport within the solar still cavity.

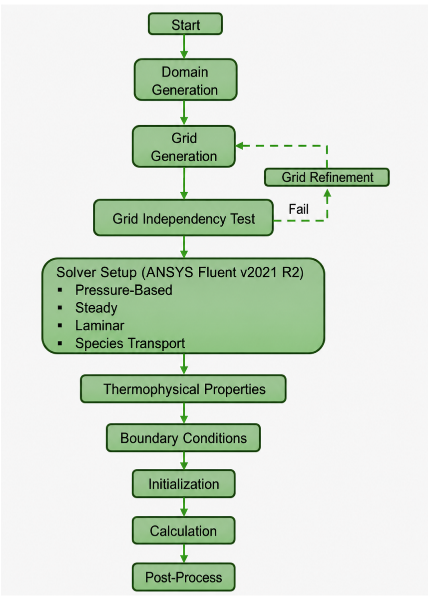

Figure 2. Framework for the numerical simulation

3 Results and Discussion

Through numerical simulations, this study elucidated the fundamental interactions between cavity geometry and buoyancy-driven thermo-fluid processes, to reveal their roles in governing the heat and mass transfer characteristics of a single-slope solar still. Rather than focusing solely on freshwater productivity, the present analysis investigated the underlying thermo-fluid mechanisms responsible for the observed performance variations. By systematically comparing five glass cover inclination angles, the evolution of the internal flow structure, thermal field, convective heat transfer, and vapor transport was examined in detail. By coupling geometric analysis with thermo-fluid transport evaluation, this approach featured the role of cavity modifications in regulating evaporation–condensation interactions and their subsequent impact on solar still efficiency.

To guarantee accuracy and reliability of the simulations, a validation study was conducted by comparing it to the numerical and experimental data reported by Rahbar and Esfahani [15]. The validation focused on evaluating the average Nusselt number across five different cases. As shown in Figure 3, the results computed by the present computational fluid dynamics (CFD) model were evaluated against theoretical models including Dunkle, Chilton-Colburn, and Bulk-Motion. The Dunkle model analysis indicated that it significantly overpredicted across all cases and this deviation was due to its inherent simplifying assumptions which neglected geometric effects and bulk fluid motion. In contrast, the present CFD results showed acceptable agreement with the more rigorous Bulk-Motion and Chilton-Colburn models. Specifically, the numerical results reflected a maximum deviation of only 8.5% (and a minimum of 0.2%) compared to the Bulk-Motion model, while the error relative to the Chilton-Colburn model remained strictly between 1.5% and 15%. The numerical model captured the shifting physical mechanisms inside the cavity. The CFD results tracked the Bulk-Motion model in the initial cases. Conversely, as the effect of this bulk flow diminished in later cases, the numerical solution shifted to mirror Chilton-Colburn results.

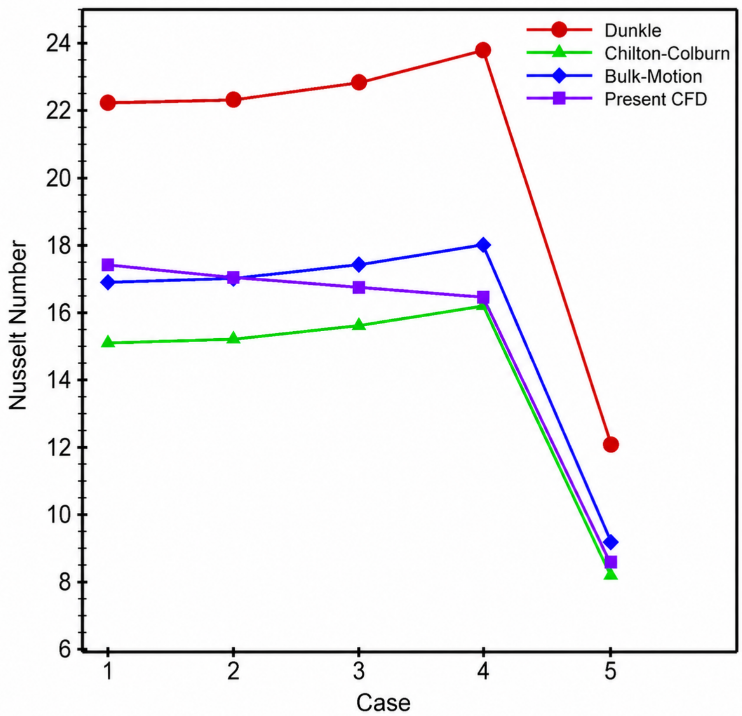

Figure 3. Validation of the present numerical model: Nusselt number variations across different models, adapted from Ref. [15]

Note: CFD—computational fluid dynamics.

The sensitivity of the solution to mesh resolution was evaluated by monitoring the primary metric of the solar still, the distillate output across a range of 1,000 to 120,000 elements. As displayed in Figure 4, computed yield has high variances at coarser grid resolutions but as the mesh becomes progressively refined, the solution stabilizes and refining the grid to 60,000 elements reduces the relative deviation to just 1.17% and less in further refinements. Therefore, to achieve balance between computational cost and numerical accuracy, a grid of 60,000 elements was selected for all parametric investigations. To maximize numerical accuracy and minimize computational cost, a structured quadrilateral mesh was employed (see Figure 5).

Figure 6 displays the temperature distribution across the five glass cover inclination angles. For the steeper angles from 15° to 30° (Figure 7b–Figure 7e), the temperature field was characterized by a single and dominant natural convection roll. In this regime, the fluid was heated at the basin, ascended toward the glass cover, and flew smoothly downward along the inclined cooling surface. However, at the shallowest angle of 10° (Figure 7a), this singular rotational flow completely broke down into multiple localized convection cells. This transition occurred because the constrained vertical cavity height restricted the global circulation loop which allowed vertical buoyancy forces to form, alongside active thermal currents of rising hot air and descending cold air.

Figure 7 shows the H_2O mass fraction contours, illustrating how water vapor is distributed within the solar still. These contours closely mirror the behavior observed in Figure 7. In the multi-cellular flow regime at 10° (Figure 8a), the transport of water vapor was localized, rising in distinct vertical streams that corresponded to the smaller convection loops. However, as the glass cover angle increased to 15° and beyond (Figure 8b–Figure 8e), the single large convection roll that swept across the entire evaporation and condensation surfaces.

Figure 8 presents the velocity magnitude contours inside the solar still across the different glass cover angles. These contours visually confirm the transition in the flow dynamics. At the lowest inclination of 10° (Figure 8a), the velocity field was divided into three distinct high-speed zones near the boundaries showing that the air-vapor mixture was circulating in three separate smaller loops. However, for angles of 15° to 30° (Figure 8b–Figure 8e), the flow changed into a single and continuous high-velocity loop wrapping around the outer edges of the cavity.

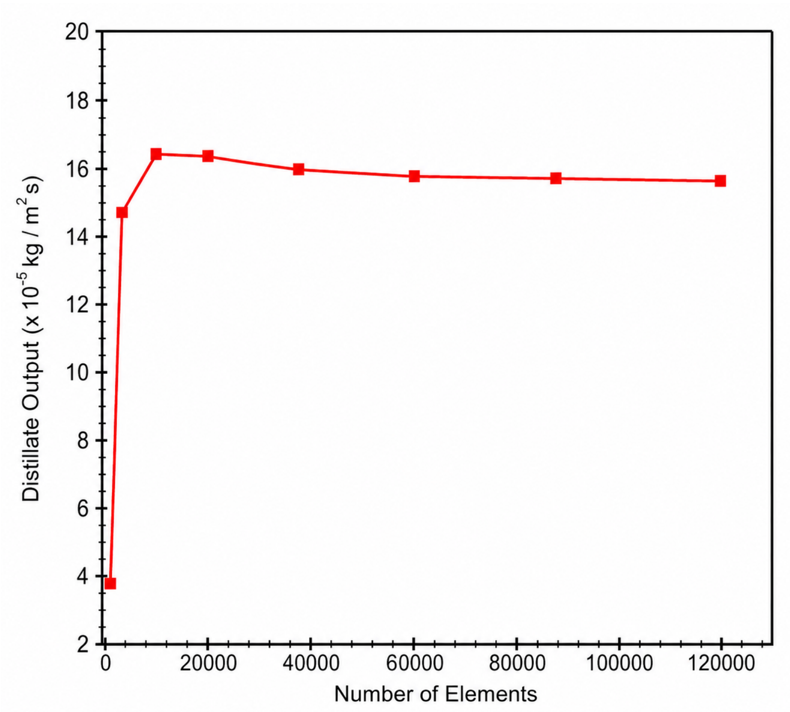

Figure 4. Grid independency

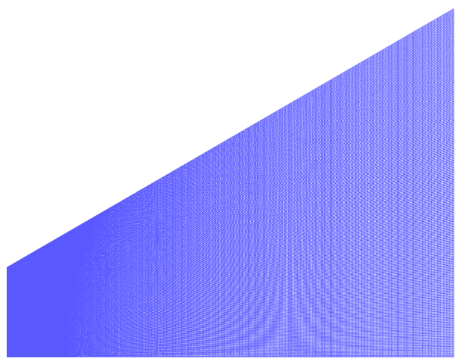

Figure 5. Structured grid of the solar still domain

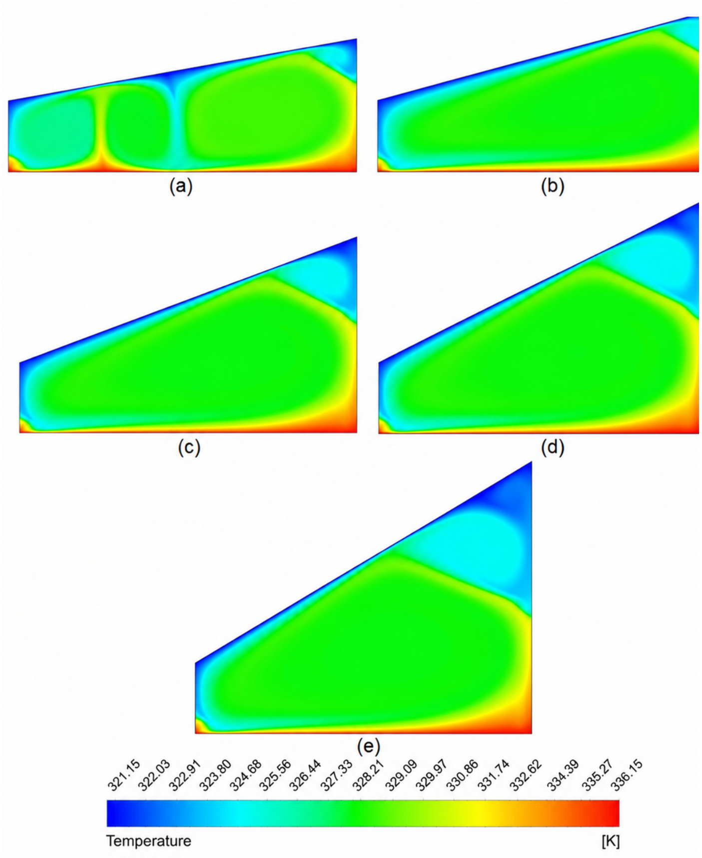

Figure 6. Temperature distribution contours for slope angles of: (a) 10°; (b) 15°; (c) 20°; (d) 25°; and (e) 30°

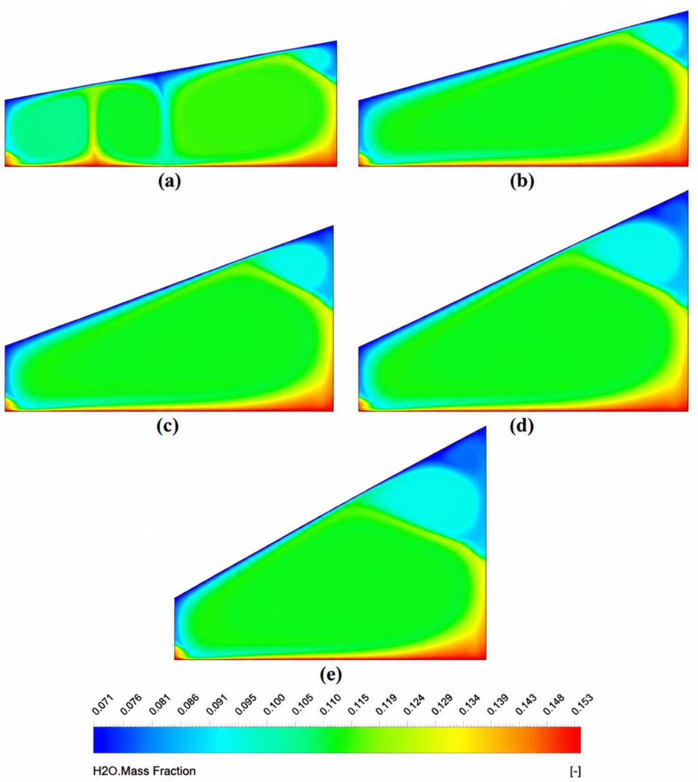

Figure 7. H_2O mass fraction contours for slope angles of: (a) 10°; (b) 15°; (c) 20°; (d) 25°; and (e) 30°

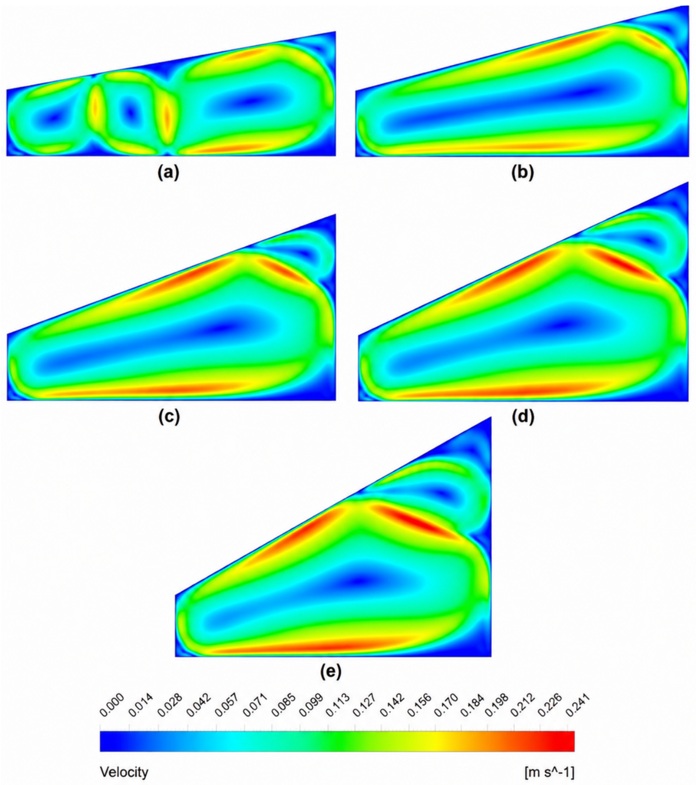

Figure 8. Velocity magnitude contours for slope angles of: (a) 10°; (b) 15°; (c) 20°; (d) 25°; and (e) 30°

To establish the relationship between the characteristics of internal flow and enhancement of heat transfer, Figure 9 depicts the local convective heat transfer coefficient along the water surface, highlighting the impact of different cavity-induced flow regimes on the thermal transport process. The data delineated a clear contrast between the multiple localized vortices and single global circulation loop flow states. For the 10° inclination, the local heat transfer coefficient featured multiple distinct peaks. These peaks corresponded directly to the impact zones of the vortices where descending cooler mixture crashed onto the hot water, thus enhancing local heat exchange. Conversely, for angles between 15° and 30°, the profiles showed a single and uniform trend. In these cases, the fluid impacts at the leading edge of the basin caused an initial peak and then swept continuously across the surface. As the air-vapor mixture travelled along the water, its thermal and concentration boundary layers thickened, resulting in a gradual decline in the heat transfer coefficient along the basin.

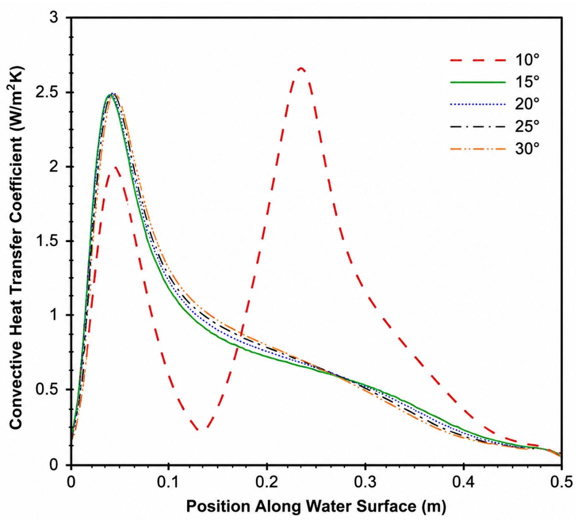

Figure 9. Variations of the local convective heat transfer coefficient along the water surface for different glass cover slope angles

Figure 10 presents the performance of the system, the total hourly yield across all five studied inclination angles. The observed trend shows that increasing the cavity height negatively influences distillate productivity, which can be attributed to the modification of internal flow behavior and the associated heat and mass transfer processes. The maximum yield is achieved at the shallowest angle of 10° which corresponds to the minimum specific height and the trend of water productivity mirrors the average convective heat transfer coefficient. Conversely, steeper glass cover inclinations enlarge the cavity height and increase the volume of the vapor space, which decreases the thermal coupling between the evaporating water surface and the condensing glass cover, thereby reducing the hourly freshwater productivity. Because making the cavity even taller no longer changes the flow, the heat transfer levels off, and the final water output stabilizes accordingly.

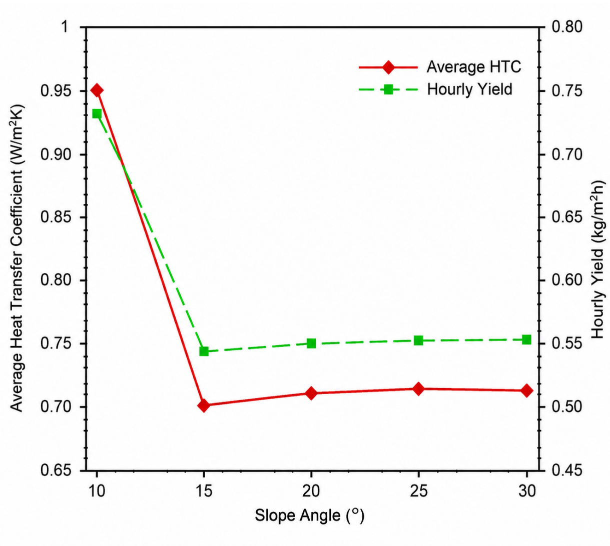

Figure 10. Correlation between the average convective heat transfer coefficient and the total hourly yield across various slope angles

Note: HTC—heat transfer coefficient.

4 Conclusions

A holistic two-dimensional numerical investigation was conducted to examine the influence of cavity geometry, represented by the glass cover inclination angle, on the thermo-fluid characteristics and freshwater productivity. Five cavity configurations with inclination angles ranging from 10° to 30° were systematically analyzed while maintaining constant basin dimensions to isolate the effect of geometry. The computational model successfully captured the interdependent effects of cavity-induced flow behavior, heat, and mass transfer characteristics, and evaporation–condensation processes inside the solar still enclosure. The outputs illustrated that the cavity geometry plays a fundamental role in determining the internal flow structure and, finally, the thermal performance of the solar still. For inclination angles between 15° and 30°, the enclosure was characterized by a single dominant natural convection cell, resulting in relatively stable circulation and a gradual reduction in the average convective heat transfer coefficient as the inclination increased. In contrast, the 10° configuration produced a markedly different flow regime, where the primary circulation divided into multiple localized convection cells. This transition enhanced fluid mixing and modified the vapor transport pathways inside the cavity. The formation of multiple vortical structures at the shallow inclination introduced the downward transport of water vapor toward the heated saline water surface, thus partitioning localized impingement regions that intensified the convective heat transfer process. The enhanced convection accelerated circulation of vapor within the enclosure and improved the evaporation–condensation cycle, hence increasing the freshwater production. The solar still with a 10° glass cover inclination achieved the highest hourly freshwater yield among all configurations under study. Furthermore, the numerical results revealed a clear correlation between freshwater productivity and the average convective heat transfer coefficient throughout the investigated inclination range. This observation confirms that the internal thermo-fluid behavior governs the overall desalination performance and highlights the importance of accurately characterizing natural convection when optimizing solar still designs.

In a nutshell, this study demonstrated that relatively simple geometric modifications could substantially alter the internal flow regime and significantly improve the thermal efficiency of passive solar desalination systems without elevating energy consumption or system complexity. The findings enlightened relevant stakeholders with innovative physical insight into the relationship between cavity geometry and transport phenomena, offering practical design guidelines for optimizing glass cover inclination to maximize freshwater production. These results established a valuable foundation for future research involving transient operating conditions, three-dimensional simulations, and experimental validation to further the advancement of high-performance solar desalination technologies.

Author Contributions

Conceptualization, A.R.N. and S.K.; methodology, A.R.N., M.J.S., and S.K.; software, A.R.N.; validation, A.R.N.; formal analysis, A.R.N. and M.J.S.; investigation, A.R.N.; writing—original draft preparation, A.R.N. and S.K.; writing—review and editing, A.R.N. and M.J.S.; visualization, A.R.N. All authors have read and agreed to the published version of the manuscript.

Data Availability

The data supporting our research results are included within the article.

Conflicts of Interest

The authors declare no conflicts of interest.

References

[1] M. Sheikholeslami and S. A. H. Hussein, "Numerical assessment of an optimized solar still integrating PCM, nanoparticles, and metal foam with reflector-based optical enhancement," *Renew. Energy*, vol. 268, p. 125637, 2026. https://doi.org/10.1016/j.renene.2026.125637

[2] Z. Esmaeili and M. Sheikholeslami, "Enhancing solar still productivity through glass cover geometry and internal baffle design: A numerical approach," *J. Water Process Eng.*, vol. 83, p. 109541, 2026. https://doi.org/10.1016/j.jwpe.2026.109541

[3] T. Elango and K. K. Murugavel, "The effect of the water depth on the productivity for single and double basin double slope glass solar stills," *Desalination*, vol. 359, pp. 82–91, 2014. https://doi.org/10.1016/j.desal.2014.12.036

[4] A. Agrawal, R. S. Rana, and P. K. Srivastava, "Heat transfer coefficients and productivity of a single slope single basin solar still in Indian climatic condition: Experimental and theoretical comparison," *Resour.-Effic. Technol.*, vol. 3, no. 4, pp. 466–482, 2017. https://doi.org/10.1016/j.reffit.2017.05.003

[5] A. Johnson, L. Mu, Y. Park, D. Valles, H. Wang, P. Xu, K. Kota, and S. Kuravi, "A thermal model for predicting the performance of a solar still with Fresnel lens," *Water*, vol. 11, no. 9, p. 1860, 2019. https://doi.org/10.3390/w11091860

[6] A. E. Kabeel, G. B. Abdelaziz, and E. M. S. El-Said, "Experimental investigation of a solar still with composite material heat storage: Energy, exergy and economic analysis," *J. Cleaner Prod.*, vol. 231, pp. 21–34, 2019. https://doi.org/10.1016/j.jclepro.2019.05.200

[7] V. K. Thakur, M. K. Gaur, A. K. Dhamneya, and M. K. Sagar, "Performance analysis of passive solar still with and without nanoparticles," *Mater. Today Proc.*, vol. 47, pp. 6309–6316, 2021. https://doi.org/10.1016/j.matpr.2021.05.539

[8] V. Nagaraju, G. Murali, A. K. Bewoor, R. Kumar, M. Sharifpur, M. El Haj Assad, and M. M. Awad, "Experimental study on performance of single slope solar still integrated with sand troughs," *Sustainable Energy Technol. Assess.*, vol. 50, p. 101884, 2021. https://doi.org/10.1016/j.seta.2021.101884

[9] H. G. Hameed, H. A. N. Diabil, and M. A. Al-Moussawi, "A numerical investigation of the enhancement of single-slope single-basin solar still productivity," *Energy Rep.*, vol. 9, pp. 484–500, 2022. https://doi.org/10.1016/j.egyr.2022.11.199

[10] F. O. Saad, S. Mankai, J. Madiouli, S. Chemkhi, I. Shigidi, and M. I. Khan, "Effect of phase change materials melting temperature on improving single slope solar still productivity," *J. Energy Storage*, vol. 97, p. 112927, 2024. https://doi.org/10.1016/j.est.2024.112927

[11] M. Abdelgaleel, E. A. AbdelAziz, H. Mosalam, A. E. Kabeel, M. Alswat, and K. Ramzy, "Investigation on the performance of modified solar distillation system using different composite materials: An experimental and theoretical study," *Solar Energy*, vol. 272, p. 112469, 2024. https://doi.org/10.1016/j.solener.2024.112469

[12] M. S. El-Sebaey, A. Hegazy, and F. A. Essa, "Performance enhancement of a tubular solar still by using stepped basins: An experimental approach," *J. Cleaner Prod.*, vol. 437, p. 140746, 2024. https://doi.org/10.1016/j.jclepro.2024.140746

[13] A. Bejan, "Mass and heat transfer by natural convection in a vertical cavity," *Int. J. Heat Fluid Flow*, vol. 6, no. 3, pp. 149–159, 1985. https://doi.org/10.1016/0142-727x(85)90002-5

[14] P. Talukdar, C. R. Iskra, and C. J. Simonson, “Combined heat and mass transfer for laminar flow of moist air in a 3D rectangular duct: CFD simulation and validation with experimental data,” *Int. J. Heat Mass Transfer*, vol. 51, no. 11–12, pp. 3091–3102, 2007. https://doi.org/10.1016/j.ijheatmasstransfer.2007.08.034
[15] N. Rahbar and J. A. Esfahani, “Productivity estimation of a single-slope solar still: Theoretical and numerical analysis,” *Energy*, vol. 49, pp. 289–297, 2012. https://doi.org/10.1016/j.energy.2012.10.023